

DiffuSent: Towards a Unified Diffusion Framework for Aspect-Based Sentiment Analysis

Shu Long^{1,2}, Yanglei Gan^{1*}, and Xuchuan Zhou³

¹ University of Electronic Science and Technology of China
yangleigan@std.uestc.edu.cn

² Southwest Petroleum University 202199010018@swpu.edu.cn

³ Southwest Minzu University xczhou@swun.edu.cn

Abstract. Aspect-Based Sentiment Analysis (ABSA) encompasses seven distinct subtasks, each focusing on different extracted elements. Despite the proven success of generative models in unified aspect sentiment analysis, existing approaches often rely on auto-regressive token-by-token generation without grasping the whole information of the aspect and opinion terms, resulting in boundary insensitivity, particularly in context of multi-word aspect and opinion terms. To address these issues, we present DiffuSent, a non-auto-regressive diffusion framework that systematically formulates all ABSA subtasks as boundary denoising diffusion processes, progressively refining boundaries over noisy states. Furthermore, we introduce a contrastive denoising training strategy which effectively address duplicate predictions with subtle variations introduced by diffusion process. Extensive experiments across 28 settings (7 subtasks \times 4 datasets) demonstrate that DiffuSent achieves delivers consistent improvements over the strongest generative and span-based systems. DiffuSent exhibits notable gains on multi-word triplets, achieving an average improvement of +2.48 F1, and maintains robust extraction accuracy in sentences containing multiple sentiment triplets. Moreover, the non-auto-regressive decoding enables substantial efficiency benefits, reaching up to $181\times$ faster inference than auto-regressive generative baselines⁴.

Keywords: Aspect-based Sentiment Analysis · Diffusion Model · Contrastive Learning.

1 Introduction

Aspect-based Sentiment Analysis (ABSA) stands as a fine-grained branch of sentiment analysis that shifts the focus from coarse document- or sentence-level sentiment to sentiment expressed toward specific entities [28]. An ABSA instance is typically composed of three essential elements: an aspect term (a), an opinion term (o), and a sentiment polarity (s). To illustrate, consider the review sentence from Res 15 shown in Figure 1, "*New hamburger with special sauce is ok at least*

* Equal contribution.

⁴ The source code is anonymous online at: <https://anonymous.4open.science/r/DiffuSent>

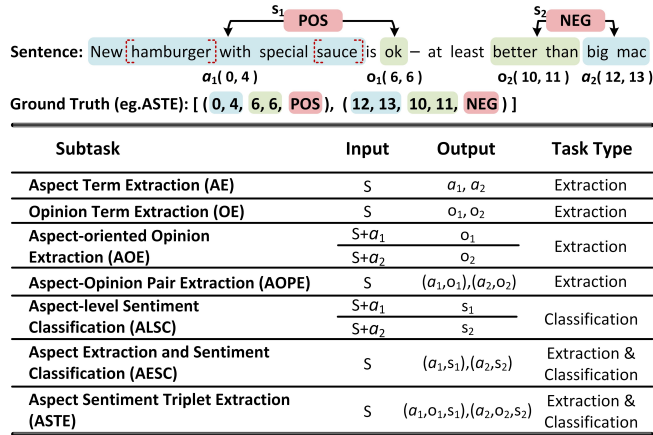


Fig. 1: Illustration of seven ABSA subtasks

better than big mac". The phrases "New hamburger with special sauce" and "big mac" function as aspect terms, while "ok" and "better than" act as opinions linked to positive/negative sentiment polarities, respectively.

Conventional approaches to ABSA have focused on distinct components such as aspect/opinion term extraction [23, 43], sentiment classification for a given aspect [32, 20], or aspect sentiment triplet extraction [25, 42, 44]. While these developments have led to successes in individual subtasks, a unified ABSA framework remains an elusive goal. To bridge this gap, recent research has been shifting towards unified approaches within a pipeline framework [24, 6]. However, such paradigms often suffer from error accumulation due to their modular approaches [7]. Addressing these drawbacks, there is a growing inclination towards employing generative models in ABSA. This shift signifies a move to an end-to-end autoregressive formulation, broadening the scope to include techniques such as word index generation [38], label augmented text generation [41], and template filling [9, 10]. Despite their effectiveness, auto-regressive generative models suffer from two critical drawbacks:

- **Boundary Ambiguity and Integrity Failure in Multi-Word Extraction.** The step-wise, token-focused mechanism of auto-regressive decoding fundamentally compromises the integrity of multi-word aspect and opinion terms. Since the model generates output sequentially, conditioning each token primarily on immediate history [1, 44], it restricts the capacity to capture the holistic context necessary for complete multi-word expressions. This often results in boundary ambiguity, where the decoder prematurely truncates a descriptive phrase, such as truncating "new hamburger with special sauce" to just "hamburger". This limitation is especially acute for long, syntactically complex, or highly descriptive aspect terms.
- **Computational Bottleneck Due to Sequential Decoding.** The inherent requirement for strictly sequential token generation in auto-regressive models

imposes a significant computational inefficiency. The decoding process enforces strict temporal dependencies, which fundamentally precludes parallel computation across the sequence length. Consequently, the inference latency scales linearly with the length of the target structured output [7, 35]. This computational cost becomes prohibitive when generating lengthy, structured outputs like multiple aspect/opinion pairs. Ultimately, this bottleneck limits the scalability of generative ABSA systems in real-world applications.

To bridge this gap, we propose DiffuSent, a novel unified generative diffusion framework tailored for ABSA. Distinct from traditional token-by-token generation paradigm, DiffuSent is designed to explicitly model boundary indices, and dynamically refines its interpretations based on comprehensive contextual information. Through a non-auto-regressive boundary denoising diffusion process, it delivers predictions for boundary indices in a single step. Specifically, we systematically infuse uncertainty via Gaussian noise into the aspect/opinion term boundaries using a forward diffusion process. The subsequent reverse diffusion process then meticulously refines these term boundaries from their initially indeterminate states. Additionally, we introduce a contrastive denoising training strategy designed to differentiate between accurate and inaccurate boundary predictions. It adeptly manages the duplicate predictions with subtle variations in boundary detection, particularly in distinguishing semantically similar terms such as "hamburger", "new hamburger", and "new hamburger with special sauce". We validate DiffuSent on four benchmarks for seven subtasks and DiffuSent yields state-of-the-art performance. Our contributions are three-fold:

- We propose DiffuSent, a unified diffusion-based framework that formulate all ABSA subtasks as boundary denoising diffusion process.
- A novel contrastive denoising training strategy is introduced. This strategy is designed to address duplicate predictions with subtle variations in predicted boundary indices introduced by diffusion process.
- Extensive experiments are conducted on 28 subtasks (7×4 datasets) to evaluate the effectiveness of our approach. Experimental results demonstrate that our model outperforms the state-of-the-art methods.

2 Related Work

Aspect-Based Sentiment Analysis (ABSA) encompasses a suite of interrelated subtasks, each focusing on specific components or their combinations within a text as illustrated in Figure 1. Previous studies mainly focus on individual subtasks [31, 34], including Aspect Term Extraction (AE), Opinion Term Extraction (OE), Aspect-level Sentiment Classification (ALSC). Subsequent research shifted towards integrated models that simultaneously extract aspects, opinions, and their corresponding sentiments [5, 8, 12], such as Aspect-oriented Opinion Extraction (AOE), Aspect-Opinion Pair Extraction (AOPE) and Aspect Extraction and Sentiment Classification (AESC). Marking a significant shift in the field, Peng *et al.* [26] introduced the Aspect Sentiment Triplet Extraction

(ASTE) task, pioneering a unified approach for extracting aspect, opinion, and sentiment triplets. This approach led to the development of advanced techniques in ABSA, such as table filling [13, 42], sequence tagging [37, 44], and span-based methods [2, 19]. However, these methods only focus on individual tasks.

Recent trends in Aspect-Based Sentiment Analysis (ABSA) have seen the emergence of unified methods, such as two-step MRC approach [24]. However, this method suffers from error accumulation due to isolated processing. In response, a shift towards end-to-end generative methods has occurred, addressing all ABSA subtasks more effectively. These include approaches like word index generation [38], label augmented text generation [41], and template filling [9, 10, 44]. However, a notable limitation of these generative models is their reliance on auto-regressive, token-by-token decoding. This approach, while effective, does not fully capitalize on the semantics available in multi-word terms and can be inefficient time-wise. In our work, we utilize a diffusion model to facilitate progressive refinements of term boundaries and output all predictions simultaneously in non-auto-regressive manner, effectively addressing complex linguistic structures. For a thorough treatment of Diffusion Model, refer to Appendix.

3 Methodology

3.1 Problem Definition

Given a sentence $S = \{w_1, w_2, \dots, w_M\}$, the objective of ASTE is to extract the boundary indices of all conceivable aspect terms, associated opinion expression terms, and their corresponding sentiment polarity labels, denoted as $T = \{(a_i^s, a_i^e, o_i^s, o_i^e, s_i)\}_{i=1}^N$. The superscripts s and e denote the start and end indices of aspect or opinion terms within the input text. The sentiment polarity label s_i takes values from $\{\text{POS}, \text{NEU}, \text{NEG}\}$, and N signifies the count of target triples. We define boundary sequences as $T_b = \{(a_i^s, a_i^e, o_i^s, o_i^e)\}_{i=1}^N$ to facilitate the subsequent presentation.

3.2 Boundary Denoising Diffusion Process

As shown in Figure 2, in our boundary denoising diffusion process, the boundary sequences T_b are considered as data samples. During the forward diffusion phase, Gaussian noise is incrementally added to indices in these sequences. Conversely, the reverse diffusion process aims to restore the original boundary indices.

Boundary Indices Forward Diffusion. In this phase, we progressively introduce Gaussian noise to the boundary sequences $T_b \in \mathbb{R}^{N \times 4}$, simulating the uncertainty inherent in identifying term boundaries. To facilitate parallel training, we normalize the count N of T_b to N_{train} by duplicating, with normalized sequences represented as $\mathbf{x}_0 \in \mathbb{R}^{N_{train} \times 4}$. The noisy sequences at any given timestep t are calculated using a one-step Markov transition as:

$$\mathbf{x}_t = \sqrt{\bar{\alpha}_t} \mathbf{x}_0 + \sqrt{1 - \bar{\alpha}_t} \epsilon \quad (1)$$

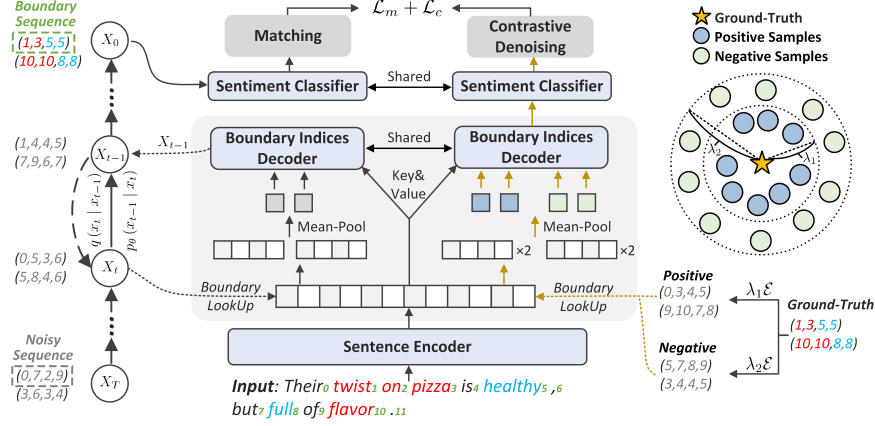


Fig. 2: Overview of DiffuSent. "Boundary LookUp" denotes get corresponding word embedding with boundary as index. The stream identified with " \uparrow " only occurs in the last reverse process in training stage and does not exist in inference stage. Noise $\mathcal{E} \sim \mathcal{N}(\mathbf{0}, \mathbf{I})$.

where $\epsilon \sim \mathcal{N}(\mathbf{0}, \mathbf{I})$ denotes the noise sampled from Gaussian distribution.

Boundary Indices Reverse Diffusion. Starting from a noise-perturbed state, the reverse diffusion process employs the non-Markovian denoising strategy DDIM [29, ?]. DDIM is for precise reconstruction of term boundaries. The process involves selecting a subsequence τ from the full timestep sequence $[1, \dots, T]$, with a length of γ . We iteratively refining the boundary sequences \mathbf{x}_{τ_i} using the information from the preceding timestep. The iterative refinement process, utilizing a trainable denoising network f_θ conditioned on S at τ_i , as follows:

$$\hat{\mathbf{x}}_0 = f_\theta(\mathbf{x}_{\tau_i}, S, \tau_i); \quad \hat{\epsilon}_{\tau_i} = \frac{\mathbf{x}_{\tau_i} - \sqrt{\alpha_{\tau_i}} \hat{\mathbf{x}}_0}{\sqrt{1 - \alpha_{\tau_i}}} \quad (2)$$

where $\hat{\mathbf{x}}_0$ denotes the predicted boundary at timestep τ_i , and $\hat{\epsilon}_{\tau_i}$ denotes the estimated noise. This noise is determined as the normalized difference between the perturbed boundary sequences \mathbf{x}_{τ_i} and the predicted boundary sequences $\hat{\mathbf{x}}_0$. The refined predictions are then combined with the estimated noise, adjusted by their respective standard deviations. This process is iteratively repeated, as encapsulated in the expression, $\mathbf{x}_{\tau_{i-1}} = \sqrt{\alpha_{\tau_{i-1}}} \hat{\mathbf{x}}_0 + \sqrt{1 - \alpha_{\tau_{i-1}}} \hat{\epsilon}_{\tau_i}$. Following γ iterations of the DDIM, the perturbed boundary indices undergo a gradual refinement, converging towards accurate boundary indices.

3.3 Network Architecture

Our denoising network $f_\theta(\mathbf{x}_t, S, t_i)$ is designed to take perturbed boundary sequences \mathbf{x}_t and the sentence S as input, and subsequently predict the corresponding term boundary $\hat{\mathbf{x}}_0$ along with the sentiment polarity. The architecture

of this network, illustrated in Figure 2, comprises two key components: a sentence encoder and a boundary indices decoder.

Sentence Encoder. The Sentence Encoder transforms the input context $S = \{w_1, w_2, \dots, w_M\}$, with a length of M , into a h -dimensional sentence representation $\mathbf{H}_S = \{h_1, h_2, \dots, h_M\} \in \mathbb{R}^{M \times h}$. Our implementation involves leveraging pre-trained language models (PLMs) [3] with a bi-directional LSTM:

$$\mathbf{H}_S = \text{Encoder}(S) \quad (3)$$

Boundary Indices Decoder. The boundary indices decoder processes the sentence representation \mathbf{H}_S to derive semantic representations for the corrupted sequence of boundary indices \mathbf{x}_t , which denote aspect and opinion terms. Initially, the noisy sequences are discretized into word indices through rescaling. The sequence representation $\mathbf{H}_X = \{h_i^X\}_{i=1}^{N_{train}} \in \mathbb{R}^{N_{train} \times h}$ is then computed by mean-pooling over the tokens at the designated start and end indices of aspect and opinion terms. Each h_i^X represents the pooled representation of the i -th sequence within boundary sequences, calculated as follows:

$$h_i^X = \text{Pooling}(h_{a_i^s}, h_{a_i^e}, h_{o_i^s}, h_{o_i^e}) \quad (4)$$

To further refine sequence representations, we utilize a transformer decoder [33] integrated with self-attention and cross-attention layers. The self-attention module enhances interactions among sequences by utilizing query, key, and values derived from the sequence representations \mathbf{H}_X :

$$\mathbf{H}_{sa} = \text{SelfAttention}(\mathbf{H}_X) \quad (5)$$

where $\mathbf{H}_{sa} \in \mathbb{R}^{N_{train} \times h}$. In tandem, the cross-attention mechanism further refines the sequence representation by incorporating the broader semantic context of the sentence. This is achieved by utilizing the output of the self-attention module \mathbf{H}_{sa} as a query, with the key and value derived from the sentence representation \mathbf{H}_S :

$$\mathbf{H}_{ca} = \text{CrossAttention}(\mathbf{H}_{sa}, \mathbf{H}_S) \quad (6)$$

where $\mathbf{H}_{ca} \in \mathbb{R}^{N_{train} \times h}$. To accommodate the iterative nature of the diffusion process, sinusoidal embeddings \mathbf{E}_t corresponding to each timestep t are integrated into the sequence representations. The final noisy sequence representations $\bar{\mathbf{H}}_X$ are calculated as follows:

$$\bar{\mathbf{H}}_X = \mathbf{H}_{ca} + \mathbf{E}_t \quad (7)$$

Moreover, we employ 4 index pointers to predict boundary indices of aspect and opinion terms, respectively. For each index $\delta \in \{a^s, a^e, o^s, o^e\}$, we create a fused representation $\mathbf{H}_{SX}^\delta \in \mathbb{R}^{N_{train} \times M \times h}$, which combines the noisy sequence representation with the sentence representation. The likelihood $\mathbf{P}^\delta \in \mathbb{R}^{N_{train} \times M}$ of each index being a boundary of term is as follows:

$$\mathbf{H}_{SX}^\delta = \mathbf{W}_S^\delta \mathbf{H}_S + \mathbf{W}_X^\delta \bar{\mathbf{H}}_X; \quad \mathbf{P}^\delta = \text{FFN}(\mathbf{H}_{SX}^\delta + \mathbf{E}_p^\delta) \quad (8)$$

where $\mathbf{W}_S^\delta, \mathbf{W}_X^\delta \in \mathbb{R}^{h \times h}$ are learnable matrices, and $FFN(\cdot)$ denotes a feed-forward network (FFN). $\mathbf{E}_p^\delta \in \mathbb{R}^{N_{train} \times M \times h}$ represents type embeddings that distinguish between aspect and opinion boundaries.

Sentiment Classifier. The sentiment classifier processes the sequence representations $\bar{\mathbf{H}}_X$ through a FFN to output a probability distribution:

$$\mathbf{P}^c = FFN(\bar{\mathbf{H}}_X) \quad (9)$$

Where, $\mathbf{P}^c \in \mathbb{R}^{N_{train} \times C}$, and C represents the total number of sentiment polarity categories.

Contrastive Denoising Training. In DiffuSent, the diffusion process introduces uncertainty, which can lead to duplicate predictions around the ground-truth boundary indices [14, 4]. This uncertainty allows the model to explore multiple plausible start and end positions, which is beneficial for multi-word terms, but it can also cause inaccurate boundary predictions under subtle variations. To improve boundary localization and reduce false triplet generation in sentiment classification, we introduce a contrastive denoising training strategy. As shown in Figure 2, we construct positive and negative samples by adding two noise scales, λ_1 and λ_2 , to the N_{train} gold boundary sequences, where $\lambda_1 < \lambda_2$. During reverse diffusion, the decoder takes both types of samples as additional inputs. Positive samples, corrupted with noise smaller than λ_1 , are expected to reconstruct the corresponding ground truth. Negative samples, corrupted with noise larger than λ_1 but smaller than λ_2 , are expected to be classified as “Invalid”, denoted by ε . For each ground-truth boundary sequence, we generate one positive and one negative sample, yielding $2 \times N_{train}$ samples per sentence. This process produces the boundary probabilities $\bar{\mathbf{P}}^\delta$ for positive samples, and the classification probabilities $\bar{\mathbf{P}}^c$ and $\tilde{\mathbf{P}}^c$ for positive and negative samples, respectively.

3.4 Training Loss

Matching Loss. To optimally align the N_{train} predictions and their corresponding N_{train} expanded ground-truth values, we employ the Hungarian algorithm [15] to establish an optimal matching $\hat{\psi}$ between the two sets. In this context, $\hat{\psi}(i)$ denotes the ground-truth corresponding to the i -th noisy sequence. The reverse process is trained by maximizing the likelihood of the prediction:

$$\mathcal{L}_m = - \sum_{i=1}^{N_{train}} \left[\sum_{\delta \in \{a^s, a^e, o^s, o^e\}} \log \mathbf{P}_i^\delta(\hat{\psi}^\delta(i)) + \log \mathbf{P}_i^c(\hat{\psi}^c(i)) \right] \quad (10)$$

Contrastive Denoising Loss. The contrastive loss consists of boundary loss and sentiment classification loss. Specifically, the boundary loss is only calculated according to boundary probabilities $\bar{\mathbf{P}}^\delta$ of positive samples. The classification loss is calculated according to classification probabilities $\bar{\mathbf{P}}^c$ and $\tilde{\mathbf{P}}^c$ for positive and negative samples, respectively. The contrastive loss is computed as:

$$\mathcal{L}_c = - \sum_{i=1}^{N_{train}} \left(\sum_{\delta \in \{a^s, a^e, o^s, o^e\}} \log \bar{\mathbf{P}}_i^\delta(\hat{Y}_i^\delta) + \log \bar{\mathbf{P}}_i^c(\hat{Y}_i^c) + \log \tilde{\mathbf{P}}_i^c(\varepsilon) \right) \quad (11)$$

We jointly optimize matching loss \mathcal{L}_m and contrastive denoising loss \mathcal{L}_c . The overall training loss is denoted as:

$$\mathcal{L} = \mathcal{L}_m + \mathcal{L}_c \quad (12)$$

4 Experiment

4.1 Experimental Setup

Datasets. We evaluate our methods across seven subtasks using four datasets from SemEval Challenges. The D_{17} dataset, annotated by [34], comprises unpaired opinion terms, while the D_{19} dataset, annotated by [5], pairs opinion terms with corresponding aspects. Annotated by [26], the D_{20a} dataset includes aspect labels, corresponding opinion labels, and sentiment polarities. Additionally, the D_{20b} dataset, refined by [37], eliminates triples with inaccurate sentiments and labels missing triples. We present their statistics in Appendix.

Baselines. The baselines for evaluating DiffuSent across various datasets are categorized into three groups:

- For AE, OE and ALSC subtasks on D_{17} , and AOE subtasks on D_{19} , the models include: BART-GEN [38], SyMux [6], SK2 [17], MvP [10].
- For AESC, AOPE, ASTE subtasks on D_{20a} , the models are Peng-two-stage [26], Dual-MRC [24], BART-GEN [38], LEGO-ABSA [9], SyMux [6], SK2 [17], MvP [10], PT-GCN [27], SAAG [30], LLaMA3-8B⁵, GPT-4o⁶.
- For ASTE subtask on D_{20b} , the baselines are BART-GEN [38], Span-ASTE [36], UIE [22], SK2 [17], SBN [2], STAGE [19], SimSTAR [16], SLGM [44], MvP [10], SATPC [18], SSGCN [40], QAIE [21], DiffuSyn [39].

4.2 Main Results

We adopt F1-score as the evaluation metric for all experiments. A predicted ABSA tuple is regarded as correct only under exact match with the gold tuple in all its elements. We make the following observations.

- **DiffuSent delivers consistent improvements across AESC, AOPE, and ASTE subtasks on D_{20a} .** As shown in Table 1, DiffuSent achieves state-of-the-art performance in all twelve settings. Relative to the strongest unified baselines per column, DiffuSent achieves improvements between 0.07 and 1.21 F1-scores, with an average gain of roughly 0.6. All reported improvements are statistically significant under a paired bootstrap test at $p < 0.01$. These results highlight that progressive boundary denoising effectively sharpens aspectopinion span localization under the exact-match criterion.

⁵ <https://huggingface.co/meta-llama/Meta-Llama-3-8B>

⁶ <https://openai.com/index/hello-gpt-4o/>

Table 1: Comparison F1-scores(%) for AESC, AOPE and ASTE on D_{20a} dataset. The best and the second best F1-scores are in **bold** and underlined, respectively. † denotes the reproduced result using the released code. Results marked with ♣ results are retrieved from [11]. Results marked with "*" indicate a statistically significant improvement with $p < 0.01$ under the bootstrap paired t-test.

Model	PLM	Lap14			Res14			Res15			Res16		
		AESC	AOPE	ASTE	AESC	AOPE	ASTE	AESC	AOPE	ASTE	AESC	AOPE	ASTE
Dual-MRC	Bert-base	64.59	63.37	55.58	76.57	74.93	70.32	65.14	64.97	57.21	70.84	75.71	67.40
SyMux	Roberta	70.32	67.64	60.11	78.68	<u>79.42</u>	<u>74.84</u>	69.08	69.82	63.13	<u>77.95</u>	78.82	72.76
SK2	Bert-large	69.42	68.12	60.14	78.72	78.19	73.32	73.30	72.05	64.32	77.78	79.89	72.03
PT-GCN	T5-base	-	-	<u>62.80</u>	-	-	74.22	-	-	67.04	-	-	<u>74.68</u>
SAAG	Bert-base	-	-	59.58	-	-	73.76	-	-	63.48	-	-	71.01
BART-GEN	Bart-base	68.17	66.11	57.59	78.47	77.68	72.46	69.95	67.98	60.11	75.69	77.38	69.98
LEGO-ABSA	T5-base	<u>72.30</u>	71.30	62.20	<u>80.60</u>	78.10	73.70	74.20	72.90	64.40	76.10	77.60	71.50
MvP†	T5-base	70.55	<u>71.38</u>	62.42	78.06	77.95	74.60	<u>74.84</u>	<u>74.06</u>	65.25	77.63	<u>80.46</u>	73.28
ChatGPT-4♣	-	52.70	42.80	-	65.93	59.70	-	65.71	55.52	-	63.38	57.93	-
ChatGPT-4o♣	-	-	-	44.63	-	-	63.57	-	-	56.53	-	-	64.68
LLaMA3-8B♣	-	-	-	36.40	-	-	53.49	-	-	46.73	-	-	56.01
DiffuSent	Bert-base	73.74*	71.67*	63.31*	81.13*	79.86*	74.91*	75.85*	74.19*	67.58*	79.16*	80.90*	75.09*

- **Superior ASTE Performance on D_{20b} Across Most Domains.** In comparison to the latest ASTE benchmarks, as shown in Table 2, DiffuSent demonstrates superior performance. Even when compared against auto-regressive generative systems including UIE, MvP, and SLGM, all of which employ the substantially larger *T5-base* backbone, DiffuSent still delivers improvements of +0.94, +0.67, and +0.81 F1 on **Res14**, **Res15**, and **Res16**, respectively. These findings confirm that our performance gains originate from the diffusion-based boundary refinement rather than from scaling pre-trained backbones.
- **Large Language Models Exhibit Systematic Weaknesses in ABSA tasks.** As reflected in Tables 1 and 2, ChatGPT-4 and ChatGPT-4o fall significantly short on all ABSA subtasks, often trailing even earlier BERT-based architectures by a considerable margin. The gap becomes especially pronounced in extraction-heavy settings such as AOPE and ASTE, where precise boundary identification and strict tuple consistency are required.
- **Consistent Advantages Across Extraction and Classification Tasks on D_{17} and D_{19} .** Figure 3 shows that DiffuSent consistently forms the outer envelope relative to representative unified baselines across AE, OE, and ALSC on D_{17} and AOE on D_{19} . This uniform dominance across both extraction-oriented tasks (AE, OE, AOE) and opinion classification (ALSC) illustrates that the underlying diffusion mechanism enhances not only boundary precision but also downstream semantic consistency.

4.3 Ablation Study

To further investigate the impact of each component and hyper-parameter in DiffuSent, we conduct comprehensive ablation studies on ASTE task on **Res15** and **Res16** from D_{20b} in Table 3.

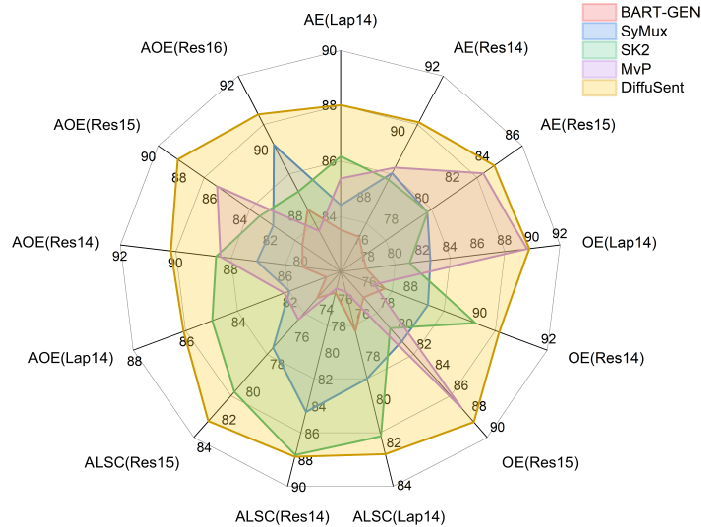


Fig. 3: Comparison F1-scores for AE, OE, ALSC on the D_{17} dataset, and AOE on the D_{19} dataset.

Contrastive Denoising. Removing the contrastive denoising (CD) objective leads to clear degradation on both datasets, with F1-score drops of 2.23 and 2.78 points on Res15 and Res16, respectively. The decline reflects the challenge posed by subtle boundary variations introduced during the diffusion process. without CD, the model more frequently produces near-duplicate spans or spurious triplets. The contrastive objective effectively suppresses these ambiguous alternatives by enforcing discriminability between clean and corrupted representations, thereby stabilizing boundary localization.

Diffusion Timestep. The diffusion timestep determines the magnitude of perturbation applied in the forward process. Table 3 shows that deviating from the default setting of 1000 timesteps in either direction harms performance. Smaller timesteps (700900) fail to introduce sufficient variation for effective denoising refinement, while larger values (15002000) inject excessive noise that obscures true boundary cues. This finding underscores that DiffuSent benefits from a moderate level of perturbation, where the injected noise is large enough to encourage robust boundary reconstruction but not so large that it overwhelms useful semantic structure.

Number of Noisy Sequence. We also vary the number of noisy sequences used during training and inference. The best performance is achieved with 60 sequences, whereas both smaller (30) and larger (90) values lead to a reduction in F1. Using too few sequences limits the model’s exposure to uncertainty, reducing its ability to generalize across boundary perturbations. Conversely, using too many sequences increases the tendency to generate redundant or varied predictions, complicating the identification of correct triplets.

Table 2: Comparison F1-scores(%) for ASTE on D_{20b} dataset. Symbols have the same meanings as in Table 1.

Model	PLM	Lap14	Res14	Res15	Res16
Span-ASTE	Bert-base	59.38	71.85	63.27	70.26
SK2	Bert-large	60.56	73.27	65.00	72.19
SBN	Bert-base	62.65	74.34	64.82	72.08
SimSTAR [†]	Bert-base	59.98	70.15	63.5	70.25
STAGE [†]	Bert-base	59.58	72.58	63.49	71.06
SATPC	Bert-base	62.59	74.79	65.03	71.17
SSGCN	Bert-base	59.74	73.05	61.74	68.57
BART-GEN	Bart-base	58.69	65.25	59.26	67.62
UIE-base	T5-base	62.94	72.55	64.41	72.86
ChatGPT-4 [♣]	-	39.01	54.89	47.88	56.55
MvP [†]	T5-base	61.51	73.48	64.65	73.38
SLGM [†]	T5-base	63.28	73.39	65.72	73.41
QAIE	T5-base	38.58	-	43.82	51.41
DiffuSyn	Bert-large	61.41	73.74	64.55	72.48
DiffuSent	Bert-base	<u>63.03*</u>	74.97*	66.39*	74.22*

Table 3: Ablation (F1-score,%) on Res15 and Res16 on ASTE subtasks. The best results are marked in **bold**.

Settings		Res15	Res16
Contrastive Denoising	X ✓	64.16 66.39	71.44 74.22
Duffusion Timestep	700	63.55	70.18
	800	64.03	72.51
	900	65.41	72.88
	1000	66.39	74.22
	1500	64.42	71.40
Number of Noisy Sequence	2000	65.57	71.22
	30	63.53	72.23
	60	66.39	74.22
	90	64.61	72.26

4.4 Performance on Multi-word Triplets

According to statistic data [44], multi-word triplets account for roughly one-third of all triplets. To assess DiffuSent’s capability with multi-word terms, we focus on triplets containing at least one multi-word aspect or opinion term, contrasting it with single-word triplets. Our evaluation includes comparisons with the latest span-based approach, STAGE [19], and a generative method, SLGM [44], on the Res15 and Res16 datasets from D_{20b} . As shown in Figure 4, our model consistently outperforms others across various metrics. Notably, DiffuSent exhibits a more substantial improvement, achieving an average F1-score increase of 2.48% for multi-word triplets compared to a 0.52% increase for single-word triplets. These results underscore DiffuSent’s effectiveness in identifying the boundaries of multi-word terms, consequently enhancing the overall performance.

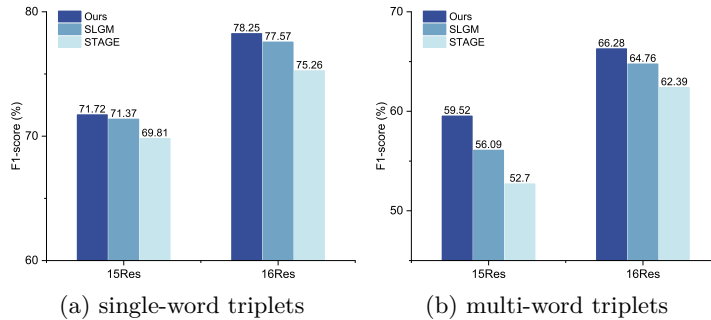


Fig. 4: F1-scores of DiffuSent on multi-word and single-word triplets compared with SLGM and STAGE.

4.5 Effective of Contrastive Denoising Scheme

Table 4 provides qualitative comparisons on Res15, illustrating how DiffuSent behaves with and without the contrastive denoising component. Across all examples, the model trained without this scheme exhibits two recurring failure modes. (i) Boundary drift induced by diffusion noise, leading to subtle but semantically consequential deviations such as predicting "bathroom" instead of the correct span "mens bathroom"; (ii) the absence of CD increases the likelihood of generating spurious triplets that do not correspond to any sentiment expression in the input sentence, thereby harming overall precision. In contrast, the full DiffuSent model reliably suppresses these erroneous alternatives and consistently recovers the correct <aspect, opinion, polarity> structure. The improvement suggests that the CD objective effectively sharpens the decision boundary between plausible and implausible span candidates by encouraging the model to contrast clean and corrupted boundary representations.

4.6 Computational Efficiency

To comprehensively evaluate the computational efficiency of DiffuSent, we compare its parameter footprint, training speed, and inference latency against state-of-the-art generative models, namely MvP and SLGM. As detailed in Table 5, DiffuSent operates with approximately half the parameters (112M) of the baselines while consistently delivering superior predictive performance. During training, DiffuSent accelerates processing by 7.77 \times compared to MvP. More notably, during inference, DiffuSent achieves a higher F1-score across all denoising timesteps (γ) while maintaining substantially higher throughput. Even under the most computationally demanding setting ($\gamma = 10$), DiffuSent achieves an F1-score of 74.3 and remains 71.5 \times and 2.5 \times faster than MvP and SLGM, respectively. This significant efficiency gain is primarily attributed to our non-autoregressive framework, which generates all triplets in parallel and effectively bypasses the bottleneck of step-by-step linearized sequence generation.

Table 4: Qualitative Comparison of DiffuSent with and without Contrastive Denoising (CD) on Noise and Boundary Resolution. ✓ indicates a correct triplet prediction, while ✗ denotes a wrong prediction. Note that spurious or extra triplet predictions are counted as incorrect, negatively impacting the overall F1-score.

Test Sentence: Oh Speaking of bathroom, the mens bathroom was disgusting.

Gold Triplet: <mens bathroom, disgusting, negative>
DiffuSent: <mens bathroom, disgusting, negative>✓
DiffuSent w/o CD: <bathroom, disgusting, negative>✓, <mens bathroom, disgusting, negative>✗

Test Sentence: Paul, the mairre d', was totally professional and always on top of things.

Gold Triplet: <Paul, professional, positive>
DiffuSent: <Paul, professional, positive>✓
DiffuSent w/o CD: <Paul, professional, positive>✓, <maitre d', professional, positive>✗

Test Sentence: The service is amazing, I've had different waiters and they were all nice, which is a rare thing in NYC.

Gold Triplet: <service, amazing, positive>, <waiters, nice, positive>
DiffuSent: <service, amazing, positive>✓, <waiters, nice, positive>✓
DiffuSent w/o CD: <service, amazing, positive>✓, <waiters, nice, positive>✓, <waiters, rare, positive>✗

Test Sentence: Shame on this place for the horrible rude staff and non-existent customer service.

Gold Triplet: <stuff, rude, negative>, <customer service, non-existent, negative>
DiffuSent: <stuff, rude, negative>✓, <customer service, non-existent, negative>✓
DiffuSent w/o CD: <stuff, rude, negative>✓, <customer service, non-existent, negative>✓, <stuff, shame, negative>✗

Test Sentence: Food was amazing - I love Indian food and eat it quite regularly, but I can say this is one of the best I've had.

Gold Triplet: <Food, amazing, positive>
DiffuSent: <Food, amazing, positive>✓, <Indian food, best, positive>✗
DiffuSent w/o CD: <Food, amazing, positive>✓, <Indian food, best, positive>✗, <Indian food, love, positive>✗, <Food, love, positive>✗

5 Conclusion

In this paper, we propose DiffuSent, a novel generative framework for unified aspect-based sentiment analysis (ABSA) that formulate all ABSA subtasks as boundary denoising diffusion process. Different from autoregressive token-by-token generation, DiffuSent explicitly models boundary indices and allows for dynamically refinements in interpreting complex linguistic structures like multi-word terms. In addition, to address duplicate predictions with subtle variations arising from diffusion process uncertainties, we design a contrastive denoising training that further refine aspect and opinion term boundaries. Experimental results demonstrate that DiffuSent yields a new state-of-the-art performance, showcasing superior performance in processing complex linguistic structures.

References

1. Cao, C., Hong, Y., Li, X., Wang, C., Xu, C., Fu, Y., Xue, X.: The image local autoregressive transformer. *Advances in Neural Information Processing Systems* **34**, 18433–18445 (2021)
2. Chen, Y., Keming, C., Sun, X., Zhang, Z.: A span-level bidirectional network for aspect sentiment triplet extraction. In: *Proceedings of the 2022 Conference on Empirical Methods in Natural Language Processing*. pp. 4300–4309 (2022)
3. Devlin, J., Chang, M.W., Lee, K., Toutanova, K.: BERT: Pre-training of deep bidirectional transformers for language understanding. In: *Proceedings of the 2019 Conference of the North American Chapter of the Association for Computational Linguistics*. pp. 4171–4186. Association for Computational Linguistics (2019)

Table 5: Computational efficiency with generative methods on **Res16** from D_{20b} . All experiments are conducted on the same setting.

	Model	Params. (Mb)	F1-score	Sents/s	SpeedUp
Training	MvP	223M	-	9.24	1.00CE
	SLGM	225M	-	41.36	4.48CE
	DiffuSent	112M	-	71.8	7.77CE
Inference	MvP	223M	73.38	0.86	1.00CE
	SLGM	225M	73.41	24.41	28.38CE
	DiffuSent _[$\gamma=1$]	112M	73.9	155.98	181.37CE
	DiffuSent _[$\gamma=5$]	112M	74.22	92.61	106.98CE
	DiffuSent _[$\gamma=10$]	112M	74.3	61.51	71.52CE

- Du, Z., Li, J.: Diffusion-based probabilistic uncertainty estimation for active domain adaptation. *Advances in Neural Information Processing Systems* **36** (2024)
- Fan, Z., Wu, Z., Dai, X.Y., Huang, S., Chen, J.: Target-oriented opinion words extraction with target-fused neural sequence labeling. In: *Proceedings of the 2019 Conference of the North American Chapter of the Association for Computational Linguistics*. pp. 2509–2518. Association for Computational Linguistics (2019)
- Fei, H., Li, F., Li, C., Wu, S., Li, J., Ji, D.: Inheriting the wisdom of predecessors: A multiplex cascade framework for unified aspect-based sentiment analysis. In: *Proceedings of the Thirty-First International Joint Conference on Artificial Intelligence, IJCAI*. pp. 4096–4103 (2022)
- Fei, H., Ren, Y., Zhang, Y., Ji, D.: Nonautoregressive encoderdecoder neural framework for end-to-end aspect-based sentiment triplet extraction. *IEEE Transactions on Neural Networks and Learning Systems* **34**(9), 5544–5556 (2023)
- Gao, L., Wang, Y., Liu, T., Wang, J., Zhang, L., Liao, J.: Question-driven span labeling model for aspect-opinion pair extraction. In: *Proceedings of the AAAI conference on artificial intelligence*. vol. 35, pp. 12875–12883 (2021)
- Gao, T., Fang, J., Liu, H., Liu, Z., Liu, C., Liu, P., Bao, Y., Yan, W.: Lego-absa: A prompt-based task assemblable unified generative framework for multi-task aspect-based sentiment analysis. In: *Proceedings of the 29th international conference on computational linguistics*. pp. 7002–7012 (2022)
- Gou, Z., Guo, Q., Yang, Y.: MvP: Multi-view prompting improves aspect sentiment tuple prediction. In: *Proceedings of the 61st Annual Meeting of the Association for Computational Linguistics*. pp. 4380–4397. Association for Computational Linguistics, Toronto, Canada (2023)
- Han, R., Peng, T., Yang, C., Wang, B., Liu, L., Wan, X.: Is information extraction solved by chatgpt? an analysis of performance, evaluation criteria, robustness and errors. *arXiv preprint arXiv:2305.14450* (2023)
- Hu, M., Peng, Y., Huang, Z., Li, D., Lv, Y.: Open-domain targeted sentiment analysis via span-based extraction and classification. In: *Proceedings of the 57th Annual Meeting of the Association for Computational Linguistics*. pp. 537–546. Association for Computational Linguistics, Florence, Italy (2019)
- Jing, H., Li, Z., Zhao, H., Jiang, S.: Seeking common but distinguishing difference, a joint aspect-based sentiment analysis model. In: *Proceedings of the 2021 Conference on Empirical Methods in Natural Language Processing*. pp. 3910–3922. Association for Computational Linguistics (2021)

14. Kou, S., Gan, L., Wang, D., Li, C., Deng, Z.: Bayesdiff: Estimating pixel-wise uncertainty in diffusion via bayesian inference. In: The Twelfth International Conference on Learning Representations (2023)
15. Kuhn, H.W.: The hungarian method for the assignment problem. *Naval research logistics quarterly* **2**(1-2), 83–97 (1955)
16. Li, D., Yang, Z., Lan, Y., Zhang, Y., Zhao, H., Zhao, G.: Simple approach for aspect sentiment triplet extraction using span-based segment tagging and dual extractors. In: Proceedings of the 46th International ACM SIGIR Conference on Research and Development in Information Retrieval. pp. 2374–2378 (2023)
17. Li, J., Zhao, Y., Jin, Z., Li, G., Shen, T., Tao, Z., Tao, C.: Sk2: Integrating implicit sentiment knowledge and explicit syntax knowledge for aspect-based sentiment analysis. In: Proceedings of the 31st ACM International Conference on Information & Knowledge Management. pp. 1114–1123 (2022)
18. Li, Q., Wen, W., Qin, J.: Improving span-based aspect sentiment triplet extraction with part-of-speech filtering and contrastive learning. *Neural Networks* **177**, 106381 (2024)
19. Liang, S., Wei, W., Mao, X.L., Fu, Y., Fang, R., Chen, D.: Stage: span tagging and greedy inference scheme for aspect sentiment triplet extraction. In: Proceedings of the AAAI Conference on Artificial Intelligence. vol. 37, pp. 13174–13182 (2023)
20. Liu, X., Hou, R., Gan, Y., Luo, D., Li, C., Shi, X., Liu, Q.: Aspect-oriented opinion alignment network for aspect-based sentiment classification. In: Proceedings of the 26th European Conference on Artificial Intelligence. pp. 1552–1559 (2023)
21. Lu, H.y., Liu, T.c., Cong, R., Yang, J., Gan, Q., Fang, W., Wu, X.j.: Qaie: Llm-based quantity augmentation and information enhancement for few-shot aspect-based sentiment analysis. *Information Processing&Management* **62**(1), 103917 (2025)
22. Lu, Y., Liu, Q., Dai, D., Xiao, X., Lin, H., Han, X., Sun, L., Wu, H.: Unified structure generation for universal information extraction. In: Proceedings of the 60th Annual Meeting of the Association for Computational Linguistics. pp. 5755–5772. Association for Computational Linguistics, Dublin, Ireland (2022)
23. Ma, D., Li, S., Wu, F., Xie, X., Wang, H.: Exploring sequence-to-sequence learning in aspect term extraction. In: Proceedings of the 57th annual meeting of the association for computational linguistics. pp. 3538–3547 (2019)
24. Mao, Y., Shen, Y., Yu, C., Cai, L.: A joint training dual-mrc framework for aspect based sentiment analysis. In: Proceedings of the AAAI conference on artificial intelligence. vol. 35, pp. 13543–13551 (2021)
25. Mukherjee, R., Nayak, T., Butala, Y., Bhattacharya, S., Goyal, P.: Paste: A tagging-free decoding framework using pointer networks for aspect sentiment triplet extraction. In: Proceedings of the Conference on Empirical Methods in Natural Language Processing. pp. 9279–9291 (2021)
26. Peng, H., Xu, L., Bing, L., Huang, F., Lu, W., Si, L.: Knowing what, how and why: A near complete solution for aspect-based sentiment analysis. In: Proceedings of the AAAI conference on artificial intelligence. vol. 34, pp. 8600–8607 (2020)
27. Peng, K., Jiang, L., Peng, H., Liu, R., Yu, Z., Ren, J., Hao, Z., Yu, P.S.: Prompt based tri-channel graph convolution neural network for aspect sentiment triplet extraction. In: Proceedings of the 2024 SIAM International Conference on data mining (SDM). pp. 145–153. SIAM (2024)
28. Pontiki, M., Galanis, D., Papageorgiou, H., Androutsopoulos, I., Manandhar, S., Mohammad, A.S., Al-Ayyoub, M., Zhao, Y., Qin, B., De Clercq, O., et al.: Semeval-2016 task 5: Aspect based sentiment analysis. In: Proceedings of the 10th International Workshop on Semantic Evaluation (SemEval-2016). pp. 19–30 (2016)

29. Song, J., Meng, C., Ermon, S.: Denoising diffusion implicit models. In: International Conference on Learning Representations (2021)
30. Sun, X., Qi, J., Zhu, Z., Li, M., Meng, J.: Senticnet and abstract meaning representation driven attention-gate semantic framework for aspect sentiment triplet extraction. *Engineering Applications of Artificial Intelligence* **139**, 109625 (2025)
31. Tang, D., Qin, B., Feng, X., Liu, T.: Effective lstms for target-dependent sentiment classification. In: Proceedings of the 26th International Conference on Computational Linguistics. pp. 3298–3307 (2016)
32. Tang, D., Qin, B., Liu, T.: Document modeling with gated recurrent neural network for sentiment classification. In: Proceedings of the 2015 conference on empirical methods in natural language processing. pp. 1422–1432 (2015)
33. Vaswani, A., Shazeer, N., Parmar, N., Uszkoreit, J., Jones, L., Gomez, A.N., Kaiser, Ł., Polosukhin, I.: Attention is all you need. *Advances in neural information processing systems* **30** (2017)
34. Wang, W., Pan, S.J., Dahlmeier, D., Xiao, X.: Coupled multi-layer attentions for co-extraction of aspect and opinion terms. In: Proceedings of the AAAI conference on artificial intelligence. vol. 31 (2017)
35. Xiao, Y., Wu, L., Guo, J., Li, J., Zhang, M., Qin, T., Liu, T.y.: A survey on non-autoregressive generation for neural machine translation and beyond. *IEEE Transactions on Pattern Analysis and Machine Intelligence* (2023)
36. Xu, L., Chia, Y.K., Bing, L.: Learning span-level interactions for aspect sentiment triplet extraction. In: Proceedings of the 59th Annual Meeting of the Association for Computational Linguistics and the 11th International Joint Conference on Natural Language Processing. pp. 4755–4766 (2021)
37. Xu, L., Li, H., Lu, W., Bing, L.: Position-aware tagging for aspect sentiment triplet extraction. In: Proceedings of the 2020 Conference on Empirical Methods in Natural Language Processing. pp. 2339–2349 (2020)
38. Yan, H., Dai, J., Ji, T., Qiu, X., Zhang, Z.: A unified generative framework for aspect-based sentiment analysis. In: Proceedings of the 59th Annual Meeting of the Association for Computational Linguistics. pp. 2416–2429 (2021)
39. Yi, Q., Kong, X., Zhu, L., Zhang, C., Shen, G.: Diffusyn: A diffusion-driven framework with syntactic dependency for aspect sentiment triplet extraction. *IEEE Transactions on Audio, Speech and Language Processing* (2025)
40. Zhang, J., Xu, S., Gao, X., Tang, Z.: Aspect sentiment triplet extraction with syntax-semantics graph convolutional network. *International Journal of Computational Intelligence Systems* **18**(1), 167 (2025)
41. Zhang, W., Li, X., Deng, Y., Bing, L., Lam, W.: Towards generative aspect-based sentiment analysis. In: Proceedings of the 59th Annual Meeting of the Association for Computational Linguistics. pp. 504–510. Association for Computational Linguistics, Online (2021)
42. Zhang, Y., Yang, Y., Li, Y., Liang, B., Chen, S., Dang, Y., Yang, M., Xu, R.: Boundary-driven table-filling for aspect sentiment triplet extraction. In: Proceedings of the 2022 Conference on Empirical Methods in Natural Language Processing. pp. 6485–6498 (2022)
43. Zhao, H., Huang, L., Zhang, R., Lu, Q., Xue, H.: Spanmlt: A span-based multi-task learning framework for pair-wise aspect and opinion terms extraction. In: Proceedings of the 58th annual meeting of the association for computational linguistics. pp. 3239–3248 (2020)
44. Zhou, S., Qian, T.: On the strength of sequence labeling and generative models for aspect sentiment triplet extraction. In: Findings of the Association for Compu-

tational Linguistics. pp. 12038–12050. Association for Computational Linguistics, Toronto, Canada (2023)